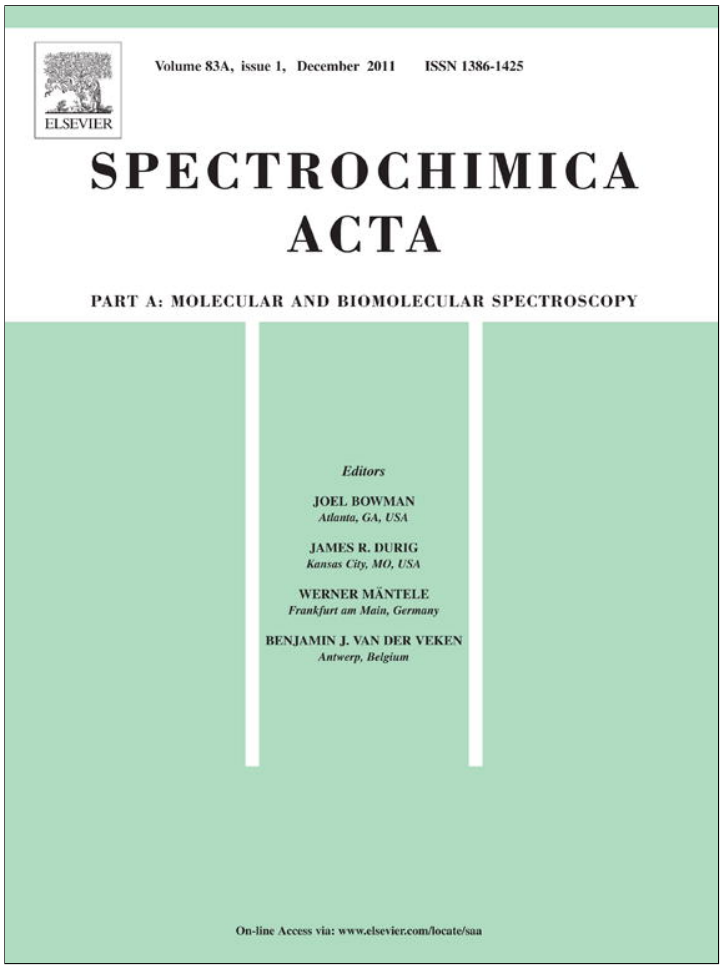

Spectrochimica Acta Part A 83 (2011) 67–73

Contents lists available at ScienceDirect

Spectrochimica Acta Part A: Molecular and Biomolecular Spectroscopy

journal homepage: www.elsevier.com/locate/saa

Structural analysis and molecular modelling of the Cu/Zn-SOD from fungal strain *Humicola lutea* 103

Pavlina Dolashka[a,*], Vesela Moshtanska[a], Aleksander Dolashki[a], Lyudmila Velkova[a], Gita Subba Rao[b], Maria Angelova[c], Christian Betzel[d], Wolfgang Voelter[e], Boris Atanasov[a,*]

[a] *Institute of Organic Chemistry, Bulgarian Academy of Sciences, G. Bonchev 9, Sofia 1113, Bulgaria*
[b] *Department of Biophysics, All India Institute of Medical Sciences, New Delhi 110029, India*
[c] *The Stephan Angeloff Institute of Microbiology, Bulgarian Academy of Sciences, Academician G. Bonchev 26, 1113 Sofia, Bulgaria*
[d] *Laboratorium für Strukturbiologie von Infektion und Entzündung DESY, Geb. 22a Nottkestr. 85–22603 Hamburg, Germany*
[e] *Interfacultary Institute of Biochemistry, University of Tübingen, Hoppe-Seyler-Strasse 4, D-72076 Tübingen, Germany*

ARTICLE INFO

Article history:
Received 2 May 2011
Accepted 13 July 2011

Keywords:
Cu/Zn-superoxide dismutase from *Humicola lutea* (HLSOD)
Circular dichroism (CD)
pH stability
Thermal stability
Thermodynamic parameters

ABSTRACT

The native form of Cu/Zn-superoxide dismutase, isolated from fungal strain *Humicola lutea* 103 is a homodimer that coordinates one Cu(2+) and one Zn(2+) per monomer. Cu(2+) and Zn(2+) ions play crucial roles in enzyme activity and structural stability, respectively. It was established that HLSOD shows high pH and temperature stability. Thermostability of the glycosylated enzyme Cu/Zn-SOD, isolated from fungal strain *H. lutea* 103, was determined by CD spectroscopy. Determination of reversibility toward thermal denaturation for HLSOD allowed several thermodynamic parameters to be calculated. In this communication we report the conditions under which reversible denaturation of HLSOD exists. The narrow range over which the system is reversible has been determined using the strongest test of two important thermodynamic independent variables (T and pH). Combining both these variables, the "phase diagram" was determined, as a result of which the real thermodynamic parameters (ΔC_p, ΔH°_{exp}, and ΔG°_{exp}) was established. Because very narrow pH-interval of transitions we assume they are as result of overlapping of two simple transitions. It was found that ΔH_o is independent from pH with a value of 1.3 kcal/mol and 2.8 kcal/mol for the first and the second transition, respectively. ΔG_o was pH-dependent in all studied pH-interval. This means that the transitions are entropically driven, these. Based on this, these processes can be described as hydrophobic rearrangement of the quaternary structure. It was also found that glycosylation does not influence the stability of the enzyme because the carbohydrate chain is exposed on the surface of the molecule.

1. Introduction

Superoxide dismutases (SODs, EC 1.15.1.1) are a family of important antioxidant metalloenzymes involved in scavenging the high level of reactive oxygen species (ROS) into molecular oxygen and hydrogen peroxide. Depending on the ions in the active site, three main metal ion forms are found in species living under very different conditions, including the deep-sea environment [1–4]. A Cu/Zn-superoxide dismutase (SOD) was characterized for the first time from *Beauveria bassiana* by gene cloning, heterogeneous expression and function analysis [5]. Several superoxide dismutases (SODs) have been identified in the genomes of: *Aspergillus fumigatus* (a cytoplasmic Cu/Zn-SOD(AfSod1p)), a mitochondrial MnSOD (AfSod2p), a cytoplasmic MnSOD (AfSod3p) and AfSod4 displaying a MnSOD C-terminal domain [6], *Spirometra erinacei* (SeCuZn-SOD) [7] or the arbuscular mycorrhizal fungus *Glomus intraradices* [8]. Another SOD containing iron (Fe–SOD) has been purified as a homodimer from *Panax ginseng* [9].

The dimeric Cu/Zn-SOD share a large structural similarity of the two monomers, such as a conserved tertiary structure and arrangement, an almost identical total number of inter- and intramolecular hydrogen bonds and salt bridges. Each monomer of SOD forms an eight-stranded Greek key β-sheet, containing an independent active site that tightly binds a catalytic copper ion and a structural zinc ion [10]. Cu/Zn-SOD is a very stable homodimeric metalloenzyme found in the yeast secretion of *Kluyveromyces lactis* [11], *Kluyveromyces marxianus* NBIMCC 1984 [12], in fungi *A. niger* 26 [13], entomogenous fungal species *Cordyceps militaris* [14], in eubacterium *Pseudoalteromonas haloplanktis* (PhSOD) [15], in

* Corresponding authors at: Institute of Organic Chemistry with Centre of Phytochemistry, Bulgarian Academy of Sciences, 9 G. Bonchev, Street, 1113 Sofia, Bulgaria. Tel.: +359 29606163; fax: +359 28700225.
E-mail addresses: pda54@abv.bg (P. Dolashka), boris@orgchm.bas.bg (B. Atanasov).

1386-1425/$ – see front matter © 2011 Elsevier B.V. All rights reserved.
doi:10.1016/j.saa.2011.07.048

freshwater mussel *Cristaria plicata* [16] or a novel psychrophilic enzyme from plant *Deschampsia antarctica*, that grows in Antarctica that survive to extreme low temperature and high UV radiation [17]. Therefore the stability of several SOD enzymes were analyzed and different methods were applied for additional stabilising the enzymes [18–20].

A positive effect on the improvement of the Cu/Zn-superoxide dismutase enzyme activity and stability as a therapeutic agent was achieved by modification of the enzyme with polysialic acids. Compared to the native enzyme, the activity and stability of the polysialylated SOD, as well as resistance to heat, acid, alkali and proteases, present in human digestive system, such as pepsin, and trypsin, were improved significantly [18]. Meantime, a dimer formation of bovine SOD-1, as well several SOD-1 mutant isoforms in humans, associated with amyotrophic lateral sclerosis, were also stabilized by mutating cysteine 111 to serine, which greatly increased the toxicity of zinc-deficient SOD [19,20].

There has been a considerable and continuing interest in the use of the antioxidant enzyme superoxide dismutase (SOD) in medicine over the last years, arising from its ability to reduce the deleterious effect of superoxide anion radicals ($^{\bullet}O^{2-}$) in the cells. One of them is a superoxide dismutase from *Humicola lutea* 103 (HLSOD) which is the first identified glycosylated fungal SOD with one mole of N-acetylglucosamine, connected to the polypeptide chain [21]. Glycosylation is very important for the function of the enzyme [22–25].

Therefore, in this study, circular dichroism was used for analyses of the reversibility and conformational stability of HLSOD under different conditions, pH and temperature, in comparison with other SODs.

2. Experimental

2.1. Purification of Cu/Zn-SOD from H. lutea

Cu/Zn-SOD was purified from the fungal strain *H. lutea* 103 from the Mycological Collection of the Institute of Microbiology, Sofia. The fermentation conditions and preparation of the purified enzyme as a water-soluble homodimeric glycoprotein with a molecular mass of approximately 31,700 Da were the same as described earlier [21]. The SOD activity was measured using the nitroblue tetrazolium (NBT) reduction method. One unit of SOD activity was defined as the amount of SOD required to inhibit the reduction of NBT by 50%, measured at 560 nm, and was expressed as units per mg protein [U/mg protein]. The protein content was estimated by the Lowry [26] procedure, using crystalline bovine serum albumin as standard.

2.2. CD measurements

Circular dichroism (CD) spectra were recorded on a J-720 dichrograph (Jasco, Tokyo, Japan). Cylindrical temperature-controlled quartz cells with a path length of 10 mm were used in all experiments. CD spectra were recorded in the range between 200 and 250 nm with a bandwidth of 1 nm, a scan speed of 50 nm/min, and a time constant of 8.0 s. The "cocktail buffer" (with constant salt concentration of 20 mM for each component) was adjusted to the given pH in the range of pH 2–12 (see below).

Protein solutions were prepared in 20 mM above described "cocktail buffer": 20 mM sodium phosphate buffer (pH 7.4–5.8), 20 mM sodium acetate buffer (pH 5.4–3.6), and 20 mM Tris–HCl buffer (6.4–11.0). The final solution mixture with protein concentration of 20 μM was incubated for 20 min at room temperature before optical measurements. Each spectrum was the average of four scans. The results were expressed as Mean Residue Ellipticity ($[\Theta]_{222}$) in deg. cm^2 dmol^{-1}.

The temperatures were thermostatically-controlled using a NESLAB thermostat model RTE-110, connected to a digital programming controller, and a thermocouple placed inside the optical cell. Two approaches were applied for evaluation of effective thermodynamic functions and determination of cross-overlapped CD data:

(1) For temperature denaturation studies, the CD spectrum of each protein sample in "cocktail" buffer of different pH values (from 1.5 to 12.0) was measured after 20 min incubation at temperatures from 20 °C up to 90 °C. The $[\Theta]_{222}$ values were recorded in intervals of 5.0 ± 0.2 °C.
(2) CD spectra of each standardized SOD solution (see above section A) were recorded at different temperatures from 20 to 90 °C (in 5 °C steps) in a wide interval of pH (4.0–11.0), with ~0.5 pH increments after incubation of 20 min. More precisely, the extreme values at 222 nm were digitalized and recalculated in $[\Theta]_{222}$ (deg cm^2 dmol^{-1}) units.

Two independent sets of experimental data were collected: (a) $[\Theta]_{222}$ as a function of T (°C) for 14 samples at different pH and (b) $[\Theta]_{222}$ as a function of pH for 15 samples at different T (°C). The experimental matrix $[\Theta]_{exp}$(T) was converted to the calculated $[\Theta]_{cal}$(pH) using data in T-dissections at different pH and the matrix $[\Theta]_{exp}$(pH) using data in pH-dissections at different temperatures – to the $[\Theta]_{cal}$(T).

The total reversibility of the system suggests independence of the final states from the path(s) of their realization. Thus, if our system is reversible, then $[\Theta]_{cal}$(T) curves must be identical to the $[\Theta]_{exp}$(T) curves and the $[\Theta]_{cal}$(pH) curves will be identical for the $[\Theta]_{exp}$(pH) curves also. To prove this strong requirement of reversibility, we have extracted each pair of curves with the same (T, pH)-signatures and plotted these as $\Delta[\Theta]$(T) and $\Delta[\Theta]$(pH) [30,34]. The relative percentage of $\Delta[\Theta]$ with steps of 4% was used to construct T-pH phase diagrams of HLSOD within 80–100% reversibility.

2.3. Estimation of the effective "melting temperatures" (T_m) and the "T_m-pH phase diagram"

From averaged $[\Theta]_{exp}$(T) curves, neglecting the complexity of the averaged curve and an oversimplified assumption for the "two-state" (N ↔ D) mechanism (crude "zero approximation"), we estimate "melting temperature" T_m [13] as the temperature of half-denaturation for SOD and thus calculate:

$$\Delta H_{eff} = \frac{4R(273 + T^{\circ}C)^2_{m,n}}{1000\,\Delta T_n\,(kcal/mol)} \quad (1)$$

Several plots were taken within the interval of pH 6.0–8.0 (region of high reversibility). All curves were symmetrical with well-defined inflexed-point of T_m. This was improved after linearization of the curves in van't Hoff's coordinates $\ln K_{obs}/R$ vs $1/T$. The slopes of these lines give the effective (van't Hoff's) enthalpies, ΔH_{vH}.

With knowledge of T_m(pH), ΔH_{vH}(pH) and C_p we are enabled to obtain pH-dependent thermodynamic stability of the protein. This was performed in the following way: T_m was used as integral characteristics of a structure containing with the expectation that there will be T/pH-dependent changes in quaternary structure. Our van't Hoff's analysis of these data was made using plots of $\log K_{obs}/R$ vs $1/T$ and calculating $\Delta G_{vh} = -RT \ln K_{obs} = -RT[Y/(1-Y)]$, where Y is the relative ($0 < Y < 1$) change of $[\Theta]_{exp}$ as a function of the temperature (in K). To compare all data to standard condition

(T_o = 298 K and $\Delta C_p = \partial \Delta H_{m,i}/\partial T_{m,i}$) the ΔG^o_{vh} was calculated using [27–29].

$$\Delta H^o_i = \Delta H_{m,i} - \Delta C_p(T_{m,i} - T_o)(\text{kcal/mol})$$

$$\Delta S^o_i = \left(\frac{\Delta H_{m,i}}{T_{m,i}}\right) - \Delta C_p \ln\left(\frac{T_{m,i}}{T_o}\right)(\text{cal/mol grad})$$

$$\Delta G^o_{vh,i} = \Delta H_{m,i}\left[1 - \left(\frac{T_o}{T_{m,i}}\right)\right] - \Delta C_p\left[(T_{m,i} - T_o) - T\ln\left(\frac{T_o}{T_{m,i}}\right)\right](\text{kcal/mol})$$

2.4. Modelling of H. lutea SOD

The sequence alignment of *H. lutea* SOD (HLSOD) with human SOD has an identity of 55.0%, which is reasonably good. The structure of HLSOD was therefore modelled using human SOD as a template. The modelling was done on a Silicon Graphics O2 workstation using the SYBYL6.81 (Tripos Inc.) molecular modelling software. The PDB file (ID 1HLS) was read in and all water molecules except the four bound waters at the active site were removed.

Based on the sequence alignment, all non-identical residues in Human SOD were mutated to those corresponding to the HLSOD sequence. Hydrogens were added and energy minimization was carried out using the Tripos Force Field with Kollman united-atom charges and a distance-dependent dielectric constant until the r.m.s. gradient was less than 0.05 kcal/mol/Å^2. During the minimization the Cu and Zn ions were kept fixed, and constraints were imposed upon the distances between Cu and its coordinating residues, Zn and its coordinating residues, and the disulfide bond between Cys57and Cys146. The minimization was found to converge in about 8000 iterations.

3. Results and discussion

In industry a major requirement for commercial SOD is thermal stability, because thermal denaturation is a common cause of enzyme inactivation. Thermostable SOD are potentially useful due to their high stability. In recent years there has been an increasing interest in SOD of thermophiles, which were expected to produce thermostable SOD. It has been reported that SOD were isolated from hyperthermophiles of the genera *Sulfolobus*, *Pyrophilus*, *Pyrobaculum* and *Aeropyrum*, but reports about SOD from thermophilic fungi are rare [30–33]. Cu/Zn-SOD from the thermophilic fungus *Chaetomium thermophilum* and *Beauveria bassiana* were expressed in *Pichia pastoris* and in *E. coli*, respectively [34,5].

Another thermostable enzyme was isolated from fungal strain *H. lutea* 103 as described before [21]. The difference of the molecular masses of *H. lutea* Cu/Zn-SOD, measured by MALDI-MS (15,935 Da) and calculated by its amino acid sequence (15,716 Da), is attributed to the carbohydrate chain of 1 mol of N-acetylglucosamine, attached to the N-glycosylation site Asn23. It was established that glycosylated HLSOD shows high pH and temperature stability, and the activity of the enzyme is about 73% after treatment with buffers at pH 6.5 and 7.8 for 1 h [21]. At pH 8.0 the enzyme activity is 10% lower and after this point remains unchanged. At low pH range (2.0–3.5) the stability is significantly lower. After treatment at a temperature of 55 °C for 1 h, the enzyme does not lose its activity, while treated at 65 °C decreases the activity to about 70% in comparison with the initial level. Here the circular dichroism was used for the study of the conformational stability of HLSOD.

It is known that most Cu/Zn-SODs possess a very compact structure that is highly resistant to denaturing agents such as urea and SDS and to attack by proteolytic enzymes. Several factors are thought to contribute to the enzyme stability, including the prosthetic metal ions, the intrasubunit disulfide bond, and the close packing of the hydrophobic interface between the subunits and the two halves of the β-sheet core. It was shown that eukaryotic Cu/Zn-SODs are characterized by a high conformational melting temperature and undergo irreversible denaturation at temperature values higher than 70 °C [35,36].

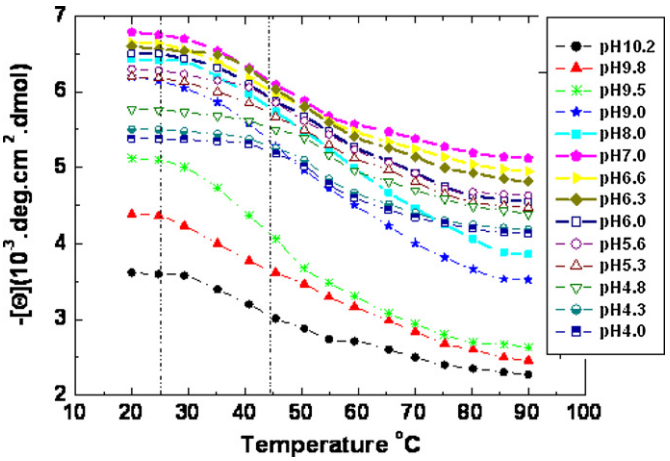

Fig. 1. Thermal unfolding, of HLSOD at same protein concentrations and buffer contents measured by circular dichroism spectra at 222 nm at different pH values. The T-induced changes are obtained over a wide temperature interval (20–90 °C). Curves considered to be reversible (solid lines) are shown within the two vertical dashed lines. All other conditions are irreversible.

3.1. Thermal stability of HLSOD in buffers with different pH

For determination of thermal stability of HLSOD, the T-transition curves at different pHs were analyzed. CD spectra of HLSOD, in cocktail buffers, were measured in the region from 200 to 250 nm and the temperature was continuously varied from 20 to 90 °C at a constant rate by adjusting the heating control of the water bath. The CD spectrum for the enzyme (pH 8.0) has 2 minima at 208 and 222 nm, which is a characteristic feature of a α-helical protein. The intermediate state relative to the native state was determined by ellipticity changes at 222 nm as a function of temperature. The initial feature of the T-transition curves is the presence of T-induced changes within a wide temperature interval (20–90 °C) (Fig. 1) and irreversibility to common "end states" with a relatively similar disordered structure.

A characteristic of reversible protein denaturation is the assumption of common end states of relatively similar disordered structures. The amplitude $\Delta[\theta]_N - \Delta[\theta]_D$ for curves at different pHs is slightly decreased for extreme pH values. The relatively small changes of the initial $[\theta]_{222}$ at high temperatures show that the main part of the structural elements are preserved, especially at neutral pH and at high temperatures. Thus, complete T-dependent unfolding was not detected and probably even at temperatures above 90 °C the structure is not a random coil (Fig. 1). The ellipticity at pH values 6–8 shows slight temperature changes. The changes at acidic range (pH 4–5.6) are smaller in comparison with the alkaline region, even at higher temperatures.

3.2. Influence of pH on the stability of HLSOD at different temperatures

The changes in the secondary structure of HLSOD at different temperatures (20–90 °C) as a function of pH (pH 4–11) were followed by near UV-CD measurements in the region between 200 and 250 nm. The $[\theta]_{222}$ vs. pH plots, shown in Fig. 2, represent a set of smooth and partially bell-shaped curves with maxima between pH 6.0 and 8.0 and non-symmetric acidic and alkaline extremes,

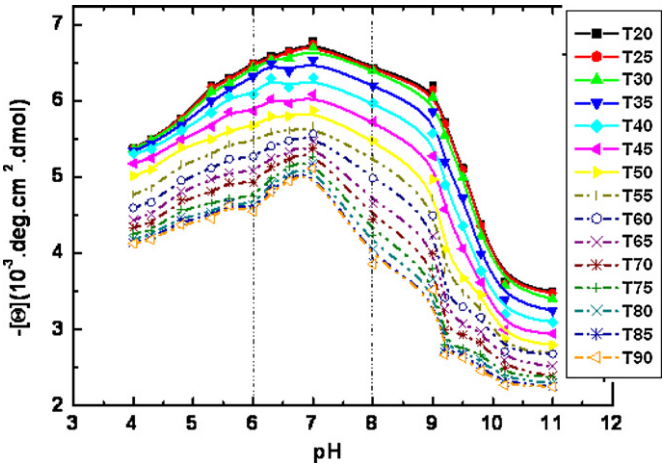

Fig. 2. Influence of pH on $[\theta]_{222}$ of HLSOD at different temperatures. Curves assumed to be reversible are locked between the dashed vertical lines.

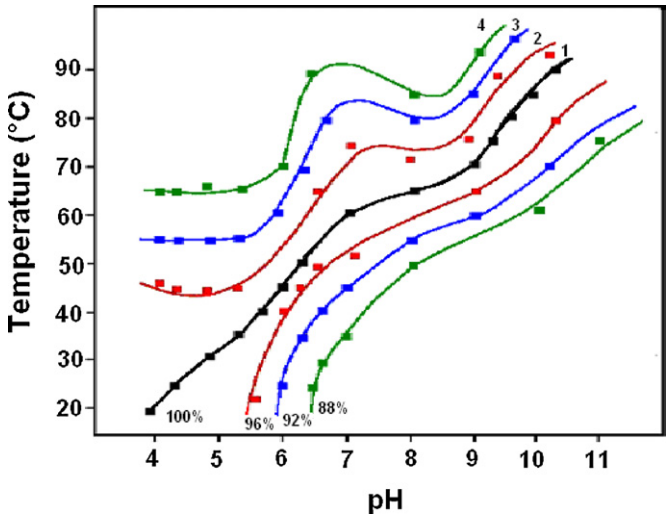

Fig. 3. "T-pH phase" diagram. Iso-lines (contours) at equal renaturation reversibility of HLSOD. The surface between T-pH lines corresponds to reversibility (in %).

but without any obvious sigmoid feature at extreme pH. In the alkaline part (pH 9–11), relative changes are too small and cooperative (within a wide pH interval), indicating that alkaline denaturation cannot be achieved as reversible process (15). In the acidic region the relative changes are smaller in comparison with the alkaline (pH 9–11) at all different temperatures. Increasing the temperatures above 65 °C, the changes in the alkaline region are well expressed, especially at pH values above 9.0.

The $[\theta]_{222}$/pH plot within the range of pH 6.0–8.0 is present for low temperatures 20–65 °C and the corresponding $[\theta]_{222}$(pH) curves are slightly pH-dependent. The conclusion is that no titrable groups of HLSOD were observed in this pH region which is responsible for structural stability. Increasing the temperature (65–90 °C), the character of the $[\theta]_{222}$(pH) curves are changed. At temperatures above 60 °C in the same pH-region the pH-dependence is increased. For the pH range (6.0–8.0), the presence of a slight peak (pH 7.0) was observed at higher temperatures (65 °C and above), indicating the presence of two ionization processes (due to carboxylate and imidazole moieties), with an opposing influence on left (L) and right (R) limbs of $[\theta]_{222}$(pH) [15]. The relatively small changes of initial $[\theta]_{222}$(pH) at high temperatures indicate that many secondary structure elements are preserved, especially at neutral pH and even at extreme high temperatures. Thus we have not detected T-dependent unfolding and probably even at temperatures above 90 °C.

3.3. T–pH reversibility "phase diagram"

The applicability of reversible thermodynamics approach can be used for evaluation of proteins' stability. The traditional approach to verify the accumulation of an intermediate state during protein unfolding or refolding is to compare the unfolding curves detected at different conditions sensitive to the different structural levels of a protein molecule. A "phase diagram", plotted as dependence of T-pH grid of $[\theta]_{222}$, represents the pH-induced conformational changes in HLSOD (Fig. 3). Because of the large set of experimental points in the diagram, we take "dissections" at a given temperature for discrete pH values and *vice versa* (at given pH for corresponding temperatures) and have converted the data to a new pair of data sets. If the principle of thermodynamic independence of the denaturation state from the way of its achievement is correct, then we should obtain the same results. We accept that extension of the relative identity (in %) is a measure and criterion of reversibility [15]. The results from this "morphing" for HLSOD are represented as lines, connect T-pH points with equal reversibility (%) as 100 (1), 96 (2), 92 (3), 88 (4) (Fig. 3). We propose that this "phase portrait" for reversibility in pH-T perturbations for HLSOD is valid, and as it is shown, the pH system is reversible at 25 °C. Increasing temperature T from 25 °C to 60 °C the reversibility increases and "opens a window" within the range of pH 6.0–8.0.

3.4. Thermodynamic characteristics of T–pH denaturation of HLSOD

Determination of reversibility for HLSOD allowed several thermodynamic parameters to be calculated. For the region of high reversibility range (pH 6.0–8.0), several plots were analyzed within interval pH 6.0–8.0, and the inflexed-point of T_m was determined (Fig. 4A). Analyzing the width of the T-transition curves on the basis of supposed "two state mechanism" it followed that they are composed of two components and represent two recognisable temperature transitions (Fig. 4A). As a next step, the effective (van't Hoff's) enthalpies ΔH_{vH} were determined from the slopes of curves $\ln K_{obs}/R$ vs $1/T$. As shown in Fig. 4B, based on the curve at pH 6.0 (Fig. 4A) ΔH_m = 8.5 kcal/mol for the first and ΔH_m = 10.87 kcal/mol for the second temperature transition were calculated. Using the same approach, T_m and ΔH_m for all the temperature transitions for the reversible region (pH 6.0–8.0) were determined. Representative data for other curves were collected in Table 1. The CD spectrum of native SOD shows a typical negative effect at 208 nm, caused by mainly β-sheet regions. Using the appropriate software [37], 39% β-sheet and only 1.4% α-helix content were calculated. The same thermodynamic parameters at the same conditions were also determined for bovine SOD. The analysis of thermodynamic data showed that HLSOD is more stable in reversible region compared with bovine SOD.

Representative data for other curves were collected in Table 1A and B. The resulting ΔH_{vH} values are plotted as ΔH_{vH} (pH) within the pH range from 6.0 to 8.0. Full reversibility is demonstrated by the fact that all experimental determinations of ΔH_m within the pH range of 6.0–8.0 are located on a straight line, which gives the effective thermal capacity at fixed pressure ($\Delta C_p \approx \partial \Delta H_{vH}/\partial T$). The average value for the first and the second temperature transition were determined, respectively, ΔC_p(I) = 290 cal/(mol grad) and C_p(II) = 340 cal/(mol grad) (Fig. 5A and B). Both ΔH°_{exp} and ΔG°_{exp} (in kcal/mol) are recalculated for the standard temperature 298 K within the pH interval 6.0–8.0.

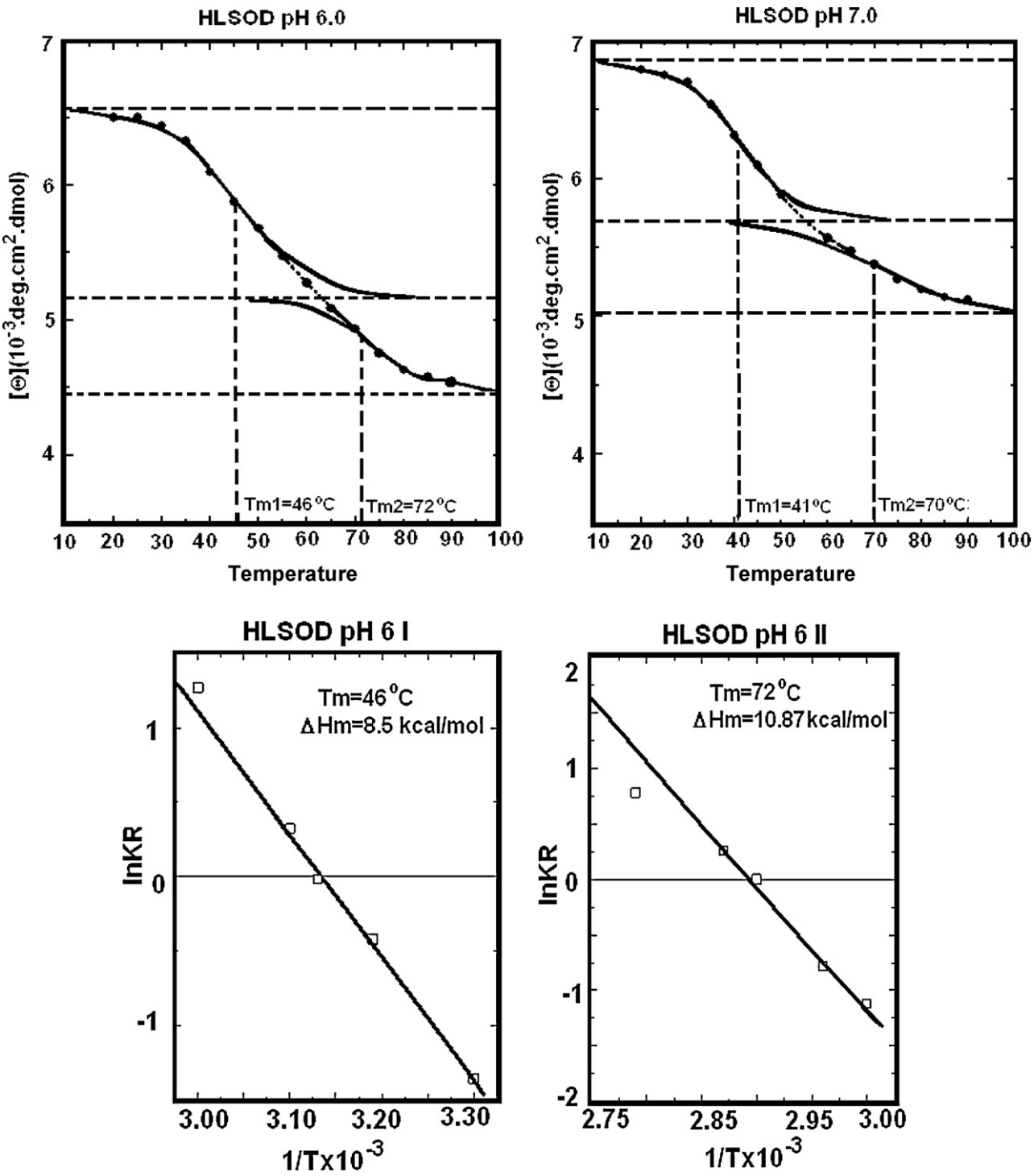

Fig. 4. (A) Plot of thermal unfolding of HLSOD in 20 mM Tris buffer, pH 6.0. (B) Linearization of the curve in van't Hoff's coordinates $\ln K_{obs}/R$ vs $1/T$. The slope of this line gives the effective enthalpy (van't Hoff's) ΔH_{vH}.

The pH-dependent part of the structural stability (ΔG°_{exp}) of reversible structural changes of HLSOD [ΔG°_{exp}(pH)] has the shape of a normal pH-dependent stability curve. After recalculation of ΔH_o from ΔH_m for each fixed pH value at standard temperature (298 K) and within the pH range of 6.0–8.0 (determined region), it was found that ΔH_o is independent of pH with a value of 1.3 kcal/mol and 2.8 kcal/mol for the first and the second transition, respectively. The fact that in the same pH-interval ΔG°_{exp} is pH-dependent followed that the entropy is the main driving force of these processes. Comparison G1- and G2-curves at Fig. 6, which are not the same, we can assume that both processes differ in changes of ionizable side chain residues indirectly involved in them. But they are not primarily responsible because the enthalpies are not pH-dependent. Therefore and most probably these processes can be described as hydrophobic rearrangement of the quaternary structure. These data are in agreement with previously published data for other fungal strain *H. lutea* 110 [1] and for new thermostable Cu/Zn SOD from a thermotolerant yeast strain *Kluyveromyces marxianus* NBIMCC 1984 [12]. The protein was characterized with some unique features such as "kinetic thermostability" ($t_{(1/2)}$ = 30 min at

Table 1
The main thermodynamic functions of reversible denaturation of (A) HLSOD and (B) SOD bovine.

I transition				II transition		
pH	ΔH_o (kcal/mol)	$\Delta S_o \times 10^{-3}$ (kcal/mol)	ΔG_o (kcal/mol)	ΔH_o (kcal/mol)	$\Delta S_o \times 10^{-3}$ (kcal/mol)	ΔG_o (kcal/mol)
SOD *Humicola lutea*						
6.0	1.4	3.6	−13.48	2.8	−1.11	−25.55
6.6	1.3	3.6	−11.02	2.8	−1.11	−23.35
7.0	1.3	3.7	−10.40	2.8	−1.11	−23.85
8.0	1.3	3.7	−12.87	2.8	−1.14	−24.33
SOD bovine						
5.6	1.2	3.72	6.34	1.2	3.48	7.59
6.0	1.2	4.00	4.96	1.2	3.35	7.31
7.0	1.3	4.16	5.91	1.3	3.72	6.57
8.0	1.2	3.57	5.44	1.2	3.33	5.06

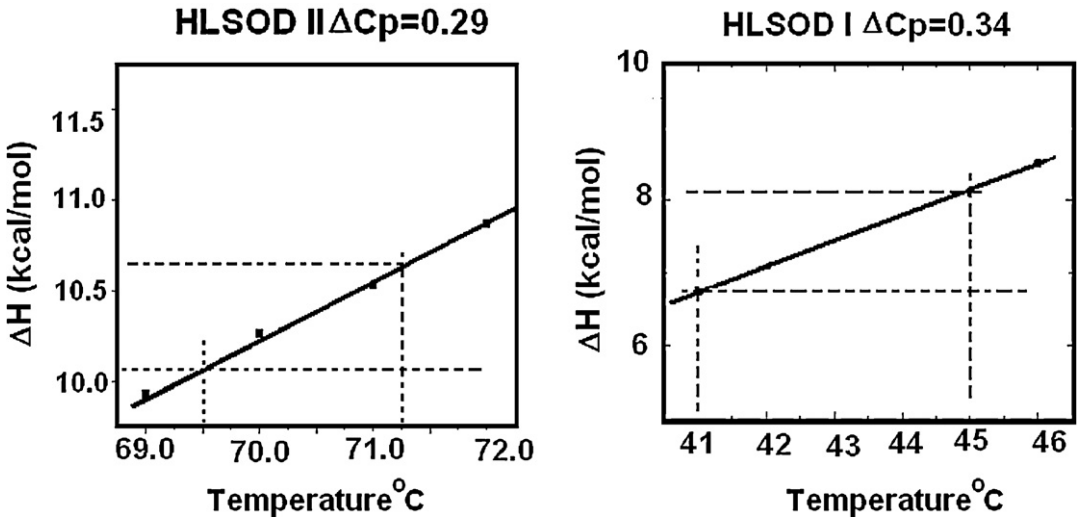

Fig. 5. Indirect determination of specific heat capacity (C_p) from ΔH_m vs T_m within the range of pH 6.0–8.0 of the denaturation process for all pH-s.

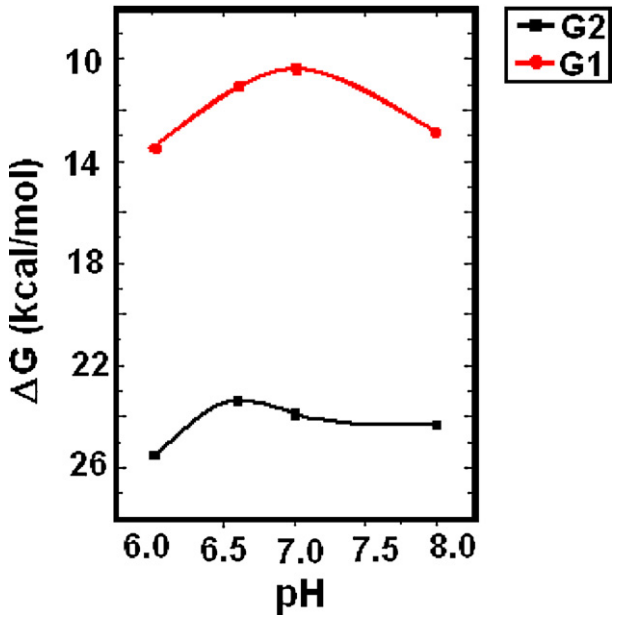

Fig. 6. The Gibbs free energy of denaturation at pH interval 6.0–8.0 (pH-dependent stability, ΔG°_{exp}) is calculated with extrapolation to $T = 298$ K. Structural stability of reversible denaturation of HLSOD is pH-dependent [ΔG°_{exp}(pH)].

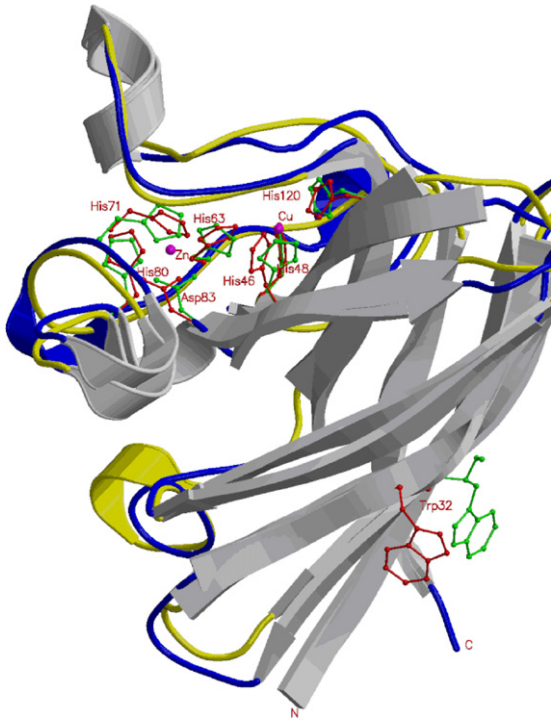

Fig. 7. Model of Cu/Zn SOD isolated from fungal strain *Humicola lutea* 103. Positions of carbohydrate chain (green) and Trp32 (red). (For interpretation of the references to color in this figure legend, the reader is referred to the web version of the article.)

70 °C) and pH stability in the alkaline range (7.5–8.5) [12]. Another enzyme isolated from entomogenous fungal species *Cordyceps militaris* has a pH optimum in the region 8.2–8.8 and remained stable at pH 5.8–9.8, 25 °C and up to 50 °C at pH 7.8 for 1.5 h incubation [14]. It was also found that a novel intracellular Cu–Zn superoxide dismutase from the freshwater mussel *Cristaria plicata* maintained more than 80% activity at temperature up to 60 °C, at pH 2.0–9.0, and was resistant to 8 M urea or 8% SDS [16].

The higher thermostability of HLSOD could be explained with the structure of the enzyme. Therefore a model was built, and the superposition of the structure of human SOD (in red) with that of HLSOD (in green) is shown in Fig. 7. The backbone r.m.s. deviation was 2.6 Å. It can be seen that the major structural changes are in the loop regions. The active site residues superimpose fairly well (the all-atom r.m.s. deviation is 0.9 Å). Also shown in Fig. 7 are the corresponding Trp32 residue and carbohydrate chain, which are different in position and in orientation. The Zn and Cu coordination and the hydrogen–bonding pattern at the active site of HLSOD are seen to be the same as in human SOD.

Finally, Fig. 7 shows the environment of the Trp residues in a sphere of 6 Å surrounding the Trp. It can notably be seen that within the dimer Trp32 of HLSOD has contacts with Ala3 and Val4 in the first β-strand as well as with Ala95 and Val96, but these do not fall within a range of 6 Å in the case of human SOD.

4. Conclusion

Structural information of HLSOD was combined with a characterization of the thermal stability of the enzyme performed by CD measurements. For the first time, we report the conditions under which reversible structural changes of HLSOD can exist. The narrow range over which the system is reversible has been determined using the strongest test of two important thermodynamic independent variables (T and pH) in a stability phase diagram, as a result of which the real thermodynamic parameters (ΔC_p, ΔH°_{exp}, and ΔG°_{exp}) were determined. In the HLSOD dimer Trp32 is close to number of hydrophobic residues (like Ala3, Val4, Ala95 and Val96) and T/pH-dependent structural rearrangement of such a hydrophobic cluster can explain the observed phenomena. The carbohydrate chain is highly exposed to the solvent and does not influence the stability of the enzyme.

References

[1] P. Dolashka-Angelova, M. Angelova, L. Genova, S. Stoeva, W. Voelter, Spectrochim. Acta A: Mol. Biomol. Spectrosc. 55A (11) (1999) 2249.
[2] E. Krumova, A. Dolashki, S. Pashova, P. Dolashka-Angelova, S. Stevanovic, R. Hristova, L. Stefanova, W. Voelter, M. Angelova, Arch. Microbiol. 189 (2007) 121.
[3] F. Guo, E. Shi-jin, S. Liu, J. Chen, D. Li, Mycologia 100 (3) (2008) 375.
[4] P.B. Stathopulos, J.A.O. Rumfeldt, G.A. Scholz, R.A. Irani, H.E. Frey, R.A. Hallewell, J.R. Lepock, E.M. Meiering, Biochemistry 12 (2003) 7021.
[5] X.Q. Xie, S.H. Ying, M.G. Feng, Enzyme Microb. Technol. 46 (3–4) (2010) 217.
[6] K. Lambou, C. Lamarre, R. Beau, N. Dufour, J.P. Latge, Mol. Microbiol. 75 (4) (2010) 910.
[7] A.H. Li, B.K. Na, S.K. Ahn, S.H. Cho, J.H. Pak, Y.K. Park, T.S. Kim, Parasitol. Res. 106 (3) (2010) 627.
[8] M. Gonzalez-Guerrero, E. Oger, K. Benabdellah, C. Azcon-Aguilar, L. Lanfranco, N. Ferrol, Curr. Genetics 56 (3) (2010) 265.
[9] Y. Hong Li, Y. Zhao, Y. Cao, N.W. Wang, D.Q. Zhao, Biomed. Chromatogr. 24 (11) (2010) 1203.
[10] I. Ascone, C. Savino, R. Kahn, R. Fourme, Acta Cryst. D66 (2010) 654.
[11] S. Raimondi, D. Uccelletti, A. Amaretti, A. Leonardi, C. Palleschi, M. Rossi, Appl. Microbiol. Biotechnol. 86 (2010) 871.
[12] T. Nedeva, P. Dolashka-Angelova, V. Moshtanska, W. Voelterm, V. Petrova, A. Kujumdzieva, J. Chromatogr. B: Anal. Technol. Biomed. Life Sci. 877 (29) (2009) 3529.
[13] R. Abrashev, S. Pashova, L. Stefanova, S. Vassilev, P. Dolashka-Angelova, M. Angelova, Can. J. Microbiol. 54 (12) (2008) 977.
[14] Z. Wang, Z. He, S. Li, Q. Yuan, Enzyme Microb. Technol. 36 (2005) 862.
[15] A. Merlino, I. Russo Krauss, I. Castellano, E. De Vendittis, B. Rossi, M. Conte, A. Vergara, F. Sica, J. Struct. Biol. 172 (3) (2010) 343.
[16] H.H. Xu, H. Ma, B.Q. Hu, D.B. Lowrie, X.Y. Fa, C.G. Wen, Fish Shellfish Immunol. 29 (4) (2010) 615.
[17] S.A. Garcıa Echauri, M. Gidekel, A. Gutierrez Moraga, L. Ordonez, G. Rojas, J.A. Contreras, A.P.B. de la Rosa, A. De Leon, Rodrıguez, Process. Biochem. 44 (9) (2009) 969.
[18] J.R. Wu, Y. Lin, Z.Y. Zheng, C.C. Lin, X.B. Zhan, Y.Q. Shen, Biotechnol. Lett. 32 (12) (2010) 1939.
[19] M. Borges-Alvarez, F. Benavente, J. Barbosa, V. Sanz-Nebot, Rapid Commun. Mass Spectrom. 24 (10) (2010) 1411.
[20] M.A. Sahawneh, K.C. Ricart, B.R. Roberts, V.C. Bombenm, M. Basso, Y. Ye, J. Sahawneh, M.C. Franco, J.S. Beckman, A.G. Estévez, J. Biol. Chem. 285 (44) (2010) 33885.
[21] P. Dolashka-Angelova, S. Stevanovic, A. Dolashki, M. Angelova, J. Serkedjieva, E. Krumova, S. Pashova, S. Zacharieva, W. Voelter, Biochem. Biophys. Res. Commun. 317 (2004) 1006.
[22] Z. Hong, P.T. Lo Verde, A. Thakur, M.L. Hammarskjold, D. Rekosh, Exp. Parasitol. 76 (2) (1993) 101.
[23] K. Arai, S. Iizuka, Y. Tada, K. Oikawa, N. Taniguchi, Biochim. Biophys. Acta 924 (1987) 292.
[24] M. Saraswathi, T. Nakanishi, A. Shimizu, Biochim. Biophys. Acta 1426 (1999) 483.
[25] S. Krantz, M. Lober, L. Henschel, Exp. Clin. Endocrinol. 88 (3) (1986) 257.
[26] O.H. Lowry, H.J. Rosenbrough, A.L. Faar, R.J. Randall, J. Biol. Chem. 193 (1951) 265.
[27] P.L. Privalov, S.J. Gill, Adv. Protein Chem. 39 (1988) 191.
[28] A. Dolashki, L. Velkova, B. Atanasov, W. Voelter, S. Stevanovic, H. Schwarz, P. Di Muro, P. Dolashka-Angelova, Biochim. Biophys. Acta 1784 (2008) 1617.
[29] P.L. Privalov, N.N. Khechinashvili, B.P. Atanasov, Biopolymers 10 (1971) 1865.
[30] S. Yamano, T. Maruyama, J. Biochem. 125 (1999) 186.
[31] S. Knapp, S. Kardinahl, N. Hellgren, G. Tibbelin, G. Schafer, R. Ladenstein, J. Mol. Biol. 285 (1999) 689.
[32] M.M. Whittaker, J.W. Whittaker, J. Biol. Inorg. Chem. 5 (2000) 402.
[33] T. Amo, H. Atomi, T. Imanaka, J. Bacteriol. 185 (2003) 6340.
[34] S. Wakadkar, L.Q. Zhang, D.C. Li, T. Haikarainen, P. Dhavala, A.C. Papageorgiou, Acta Cryst. F66 (2010) 1089.
[35] A. Battistoni, S. Folcarelli, L. Cervoni, F. Polizio, A. Desideri, A. Giartosio, G. Rotilio, JBC 273 (10) (1998) 5655.
[36] M.A. Hough, R.W. Strange, S.S. Hasnain, J. Mol. Biol. 304 (2000) 231.
[37] J.T. Yang, C.-S.C. Wu, H.M. Martinez, Methods Enzymol. 130 (1986) 208.